Stability and binding energy of small asymptotically Randall-Sundrum black holes

Scott Fraser and Douglas M. Eardley

Phys. Rev. D **92**, 024032 — Published 20 July 2015

DOI: 10.1103/PhysRevD.92.024032

Stability and binding energy of small asymptotically Randall-Sundrum black holes

Scott Fraser*
Department of Physics, California Polytechnic State University, San Luis Obispo, California 93407

Douglas M. Eardley†
Department of Physics, University of California, Santa Barbara, California 93106

We study the binding of a small black hole to a positive-tension brane in the second Randall-Sundrum scenario (RS2) with orbifold symmetry. We find that a small black hole on the brane has substantial binding energy to the brane, and is stable against escaping into the bulk. This result can be applied in other models with an orbifold-symmetric brane. We also find a novel static black hole, which is completely localized off the brane and is unstable against translations transverse to the brane. Our results are obtained analytically by applying a variational principle to black hole initial data. This paper is the second in a series on asymptotically RS black holes.

PACS numbers: 04.50.Gh, 04.70.Bw

I. INTRODUCTION

There is ongoing interest in the Randall-Sundrum (RS) models [1, 2], where our observed universe is a brane surrounded by a higher-dimensional anti-de Sitter (AdS) bulk. If the higher-dimensional Planck energy is of order TeV, an exciting prediction in the RS1 model [1] is the possible production of small black holes at TeV scale collider energies [3], and LHC experiments [4, 5] continue to test this hypothesis.

In such models, Standard Model particles are confined to the brane, while gravity (described by spacetime curvature) propagates in the bulk. A black hole is a purely gravitational object, so a natural question is whether a black hole on a brane could escape into the bulk. In the RS models, a brane has orbifold symmetry: mirror points across the brane are identified. Without orbifold symmetry, a small black hole can escape [6], possibly pinching off some of the brane [7]. Orbifold symmetry would appear to forbid such pinching off, but the question of escape has generally remained open; in this paper, we will give different arguments against escape than in [8]. For a large black hole on the brane, AdS/CFT arguments suggest that the black hole may classically evaporate by emitting gravitational waves [9] or smaller black holes [10].

The RS1 model [1] has two branes of opposite tension, with our universe on the negative-tension brane. In the RS2 model [2], our universe resides on the positive-tension brane, with the negative-tension brane removed to infinite distance. Perturbations of RS2 reproduce Newtonian gravity at large distance on the brane, while in RS1 this requires a mechanism to stabilize the inter-brane distance [11]. In RS2, solutions for static black holes on the brane have been found numerically, for both small black holes [12, 13] and large black holes [14], compared to the AdS curvature length. The only known analytic black hole solutions are the static and stationary solutions [15, 16] in a lower-dimensional version of RS2.

In this paper, we examine the binding of small black holes to a positive-tension brane with orbifold symmetry in RS2. No exact solutions are known for these black holes, and numerical methods have been essential to study them. Here, we take a different approach using our variational principle [17] for black holes in RS2:

> *Initially static initial data that extremizes the mass is initial data for a static black hole, for variations at fixed apparent horizon area A, AdS curvature length ℓ, cosmological constant Λ, brane tension λ and asymptotic warp factor ψ_0 on the brane.* (1)

Our approach is analytical. There has also been some numerical work [18] using extrema in a detuned RS2 setup.

This paper is organized as follows. We derive a general binding energy result in section II, and review the RS models in section III. We formulate our initial data in section IV, and solve the resulting boundary value problem in the following two different regimes. In section V, for small black holes on or near the brane, our variational principle reproduces the well known static braneworld black hole, which we show is translationally stable and has large binding energy to the brane. In section VI, for small black holes farther from the brane, our variational principle locates a new static black hole, which is translationally unstable. In section VII, we examine the energy and length scales for which our results are valid, and the related phenomenology. We conclude in section VIII.

We work primarily on the orbifold (one side of the brane) in $D = 5$ spacetime dimensions. Spatial geometry has metric h_{ab} and covariant derivative D_a. A spatial boundary has metric σ_{ab}, extrinsic curvature $k_{ab} = h_a{}^c D_c n_b$, and outward unit normal n_a. We often use $\simeq$ for approximations at leading order, and often refer to the black hole rest mass M_A, defined by horizon area A and area ω_{D-2} of the $(D-2)$-dimensional unit sphere,

$$M_A = \frac{(D-2)\omega_{D-2}}{16\pi G_D}\left(\frac{A}{\omega_{D-2}}\right)^{(D-3)/(D-2)} . \quad (2)$$

* Email address: scfraser@calpoly.edu
† Email address: doug@kitp.ucsb.edu

II. BINDING ENERGY: GENERAL RESULTS

Even if a brane has zero tension, it can still profoundly affect physics in the ambient spacetime, if there is an orbifold symmetry at the brane. Imposition of an orbifold symmetry decimates the degrees of freedom, and thus places great restrictions on the classical and quantum dynamics of spacetime, and of fields on spacetime. The case of interest in this paper is the $\mathbb{Z}_2$ orbifold symmetry of a RS2 braneworld in spacetime dimension $D = 5$. However, the issue is quite general, and also applies to $D > 5$, as long as orbifold symmetries hold. In this section, we give strong arguments that a small black hole has a large gravitational binding energy to such a brane.

If an asymptotically RS black hole is sufficiently small compared to the AdS curvature length ℓ, the values of brane tension and bulk cosmological constant can be neglected, since they are proportional to $1/\ell$ and $1/\ell^2$, respectively (see section III below). By neglecting the tension and cosmological constant, we will derive below a simple result for the binding energy E_B of a black hole to a tensionless brane with $\mathbb{Z}_N$ orbifold symmetry in an effectively asymptotically flat spacetime. Our derivation will assume that mass is normalized with respect to an observer on the brane. Our result (7) will give accurate results for the asymptotically RS2 geometry in this paper, and it can also be applied to an asymptotically RS1 geometry; we therefore regard (7) as a general result, valid for the specific case of sufficiently small black holes in the vicinity of the brane. In section VII, we will obtain upper bounds for the mass M and black hole area A, compared to the AdS length scale, for which the small black hole approximation is valid.

Let $\mathcal{V}$ (the bulk spacetime) be a Riemannian manifold with a submanifold $\mathcal{W}$ (the brane). Let $\mathbb{Z}_N$ be a discrete symmetry of $\mathcal{V}$ that leaves $\mathcal{W}$ fixed. All of physics is to be invariant under $\mathbb{Z}_N$. Thus, all classical solutions are symmetric under $\mathbb{Z}_N$, and all quantum states are invariant under $\mathbb{Z}_N$. We can construct classical solutions of the field equations in two ways: (a) on a manifold $\mathcal{V}$ containing N identical copies of the solution (before imposition of the orbifold symmetry); or (b) on a manifold-with-boundary or manifold-with-conical-singularity $\mathcal{V}/\mathbb{Z}_N$ (after imposition of the orbifold symmetry).

Global charges in $\mathcal{V}$ must be divided by N, when measured in the orbifolded spacetime $\mathcal{V}/\mathbb{Z}_N$. This is clear in the manifold-with-boundary view. In the orbifold view, it follows because our representation of physics is N-fold redundant. For instance, an electromagnetic charge Q in $\mathcal{V}$, away from $\mathcal{W}$, must have N copies in all; but Gauss's law should give Q, not NQ, for the total charge. If the charge lies on $\mathcal{W}$, its N copies coincide; but we must regard the total charge as Q, not NQ. Thus, in the orbifold view, the rule is to calculate charges by flux laws on large surfaces in $\mathcal{V}$, but then divide by N; this gives the same answer as from a large $\mathbb{Z}_N$ invariant surface in $\mathcal{V}/\mathbb{Z}_N$.

As measured in $\mathcal{V}$, a small nonrotating, uncharged, black hole has mass M_0 and area A_0 related by (2),

$$A_0 = c_D M_0^{(D-2)/(D-3)} \ , \tag{3}$$

with c_D a constant. To construct a braneworld black hole centered on the brane, we apply a $\mathbb{Z}_N$ symmetry, under which the black hole is invariant, as viewed in $\mathcal{V}$. As measured in $\mathcal{V}/\mathbb{Z}_N$, the black hole has mass $M_1 = M_0/N$ and area $A_1 = A_0/N$.

To construct a black hole far from the brane, it must appear in N copies, so as to be invariant under $\mathbb{Z}_N$. We cannot construct a static solution for this situation, since the black hole will be attracted by its image black holes under $\mathbb{Z}_N$. However, we can construct initially static initial data by the well known method of images [19, 20]. If the black hole is sufficiently far from the brane, the solution in a neighborhood of the black hole will be close to the solution for a single static black hole, so the black hole has mass M_2 and area A_2 related by (2),

$$A_2 = c_D M_2^{(D-2)/(D-3)} \ . \tag{4}$$

A black hole on the brane has mass $M_1 = M_0/N$ and

$$A_1 = \frac{A_0}{N} = c_D M_1^{(D-2)/(D-3)} N^{1/(D-3)} \ . \tag{5}$$

If the black hole could leave the brane in a reversible process, the area would remain constant, $A_2 = A_1$. Thus, for a reversible process,

$$M_2 = M_1 N^{1/(D-2)} \ . \tag{6}$$

If the process were irreversible, then $A_2 > A_1$, hence $M_2 > M_1 N^{1/(D-2)}$. In either case, $M_2 > M_1$, so energy would be required to drive the process. The minimum binding energy E_B of the black hole to the brane is thus

$$E_B = M_2 - M_1 = \left[N^{1/(D-2)} - 1 \right] M_1 \ . \tag{7}$$

Note that E_B is of order M_1, and hence substantial. One can interpret this result in terms of an effective binding force: if a black hole is off the brane, it experiences attractive image forces from its copies in the orbifold view. The results (6) and (7) will be borne out explicitly in the initial data that we will construct in section V.

III. THE RANDALL-SUNDRUM MODELS

The Randall-Sundrum spacetimes [1, 2] are portions of an AdS spacetime, with metric

$$ds^2_{\rm RS} = \psi_0^2 \left(-dt^2 + d\rho^2 + \rho^2 d\omega^2_{D-3} + dz^2 \right) \ . \tag{8}$$

Here $d\omega^2_{D-3}$ denotes the unit $(D-3)$-sphere. The warp factor is $\psi_0 = \ell/(\ell + z)$, where z is the extra dimension and ℓ is the AdS curvature length, related to the bulk cosmological constant Λ given below. The RS1 model [1]

contains two branes, the surfaces $z = 0$ and $z = z_c$. The bulk cosmological constant Λ and brane tensions λ_i are

$$\Lambda = -\frac{(D-1)(D-2)}{2\ell^2} \ , \quad \lambda_1 = -\lambda_2 = \frac{2(D-2)}{8\pi G_D \ell} \ . \quad (9)$$

The dimension z is compactified on an orbifold $(S^1/\mathbb{Z}_2)$ and the branes have orbifold mirror symmetry: in the covering space, symmetric points across a brane are identified. There is a discontinuity in the extrinsic curvature k_{ab} across each brane given by the Israel condition [21]. Using orbifold symmetry, the Israel condition requires the extrinsic curvature k_{ab} at each brane to satisfy

$$2k_{ab} = \left(\frac{8\pi G_D \lambda}{D-2}\right) \sigma_{ab} \ . \quad (10)$$

The RS2 spacetime is obtained from RS1 by removing negative-tension brane (now a regulator) to infinite distance ($z_c \to \infty$) and the orbifold region has $z \geq 0$.

IV. FORMULATION OF THE INITIAL DATA

Here we formulate the initial data for small initially static black holes in RS2. As described in [22], this amounts to solving the constraint $\mathcal{R} = 2\Lambda$, where $\mathcal{R}$ is the Ricci scalar of the spatial metric h_{ab}. The spatial geometry can be visualized as a conventional embedding diagram [19, 20] with two asymptotically RS2 regions (instead of asymptotically flat regions), connected by a bridge. The bridge's minimal surface is the apparent horizon, which is the best approximation to the event horizon within the spatial geometry. If the black hole is sufficiently far from the brane, we refer to the apparent horizon as the throat. If the black hole is sufficiently close to the brane, the apparent horizon is the outermost extremal surface surrounding the throat. Figure 1 illustrates the setup in convenient coordinates.

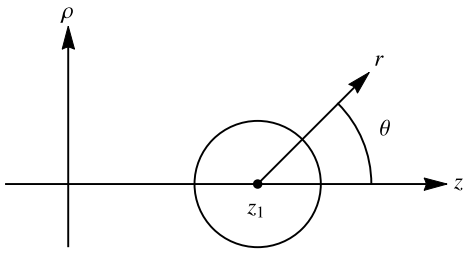

FIG. 1. The brane and black hole throat. The brane (at left) is the plane $z = 0$. The black hole throat (the circle) has radius $r = a$ in coordinates (r, θ) centered at $z = z_1$.

We use a conformally flat metric,

$$ds^2 = \psi^{4/(D-3)} d\mathbf{x}^2 \ , \quad \mathbf{x} = (\vec{\rho}, z) \ . \quad (11)$$

Here $\mathbf{x} = (\vec{\rho}, z)$ are Cartesian coordinates, with Laplacian ∇^2. The constraint is then

$$\nabla^2 \psi = \frac{(D-1)(D-3)}{4\ell^2} \psi^{(D+1)/(D-3)} \ . \quad (12)$$

This is invariant under inversion J through a sphere of radius a and center $\mathbf{C}$. J acts on $\mathbf{x}$ and functions f as

$$J\mathbf{x} = \mathbf{C} + \frac{a^2}{|\mathbf{x}-\mathbf{C}|^2}(\mathbf{x}-\mathbf{C}) \ , \quad (13a)$$

$$J[f](\mathbf{x}) = \frac{a^{D-3}}{|\mathbf{x}-\mathbf{C}|^{D-3}} f(J\mathbf{x}) \ . \quad (13b)$$

Note that J^2 is the identity, and

$$d(J\mathbf{x})^2 = \frac{a^4}{|\mathbf{x}-\mathbf{C}|^4} d\mathbf{x}^2 \ , \quad (14a)$$

$$\nabla^2 J[f] = \frac{a^4}{|\mathbf{x}-\mathbf{C}|^4} J\left[\nabla^2 f\right] \ . \quad (14b)$$

From (14b), if ψ is a solution of (12), then so is $J[\psi]$. If the inversion is an isometry of the metric (11), then

$$ds^2 = [\psi(J\mathbf{x})]^{4/(D-3)} d(J\mathbf{x})^2 \ . \quad (15)$$

By (14a), this requires $J[\psi] = \psi$, which we will impose across the throat. In the covering space, we also impose orbifold reflection isometry about the brane. Since the conformal isometries of flat space are limited to reflections and inversions, we take the brane as the coordinate plane $z = 0$ and the throat as a coordinate sphere of radius a and center $\mathbf{C} = (\vec{0}, z_1)$ in Cartesian coordinates $(\vec{\rho}, z)$. For cylindrical coordinates (ρ, z, φ_i) and spherical coordinates (r, θ, φ_i) centered at $\mathbf{C}$,

$$|\vec{\rho}| = \rho = r\sin\theta \ , \quad z = z_1 + r\cos\theta \ . \quad (16)$$

In the spherical coordinates (r, θ, φ_i), the inversion isometry condition $\psi = J[\psi]$ is

$$\psi(r, \theta, \varphi_i) = \left(\frac{a}{r}\right)^{D-3} \psi(r', \theta, \varphi_i) \ , \quad r' = \frac{a^2}{r} \ . \quad (17)$$

Our two isometries are then

$$J[\psi] = \psi \ , \quad \psi(\vec{\rho}, -z) = \psi(\vec{\rho}, z) \ . \quad (18)$$

The boundary conditions are, with $q = (D-1)/(D-3)$,

$$[2\ell\partial_z\psi + (D-3)\psi^q]\Big|_{z=0} = 0 \quad (19a)$$

$$[2r\partial_r\psi + (D-3)\psi]\Big|_{r=a} = 0 \quad (19b)$$

$$\psi \underset{|\mathbf{x}|\to\infty}{\longrightarrow} \psi_0 \ . \quad (19c)$$

The result (19a) follows from the Israel condition (10), and (19b) follows from differentiating (17).

Thus, to construct an initially static geometry for a small black hole ($a \ll \ell$), we must solve the boundary value problem consisting of (12), (18), and (19). We will solve this outside of the throat. Inversion could then be used to extend the solution inside the throat, if desired.

Although (12) and (19a) are nonlinear, this system should be solvable, since ψ should interpolate between

two known solutions: far from the apparent horizon, ψ approaches the RS solution (8), while near the apparent horizon, the AdS curvature has little effect and ψ approaches the D-dimensional Schwarzschild solution.

We will solve the above boundary value problem in the next two sections, in two different regimes: in section V, the black hole is on or near the brane, and in section VI, the black hole is farther from the brane.

V. BLACK HOLES NEAR THE BRANE

Here we solve the boundary value problem of section IV, for small black holes ($a \ll \ell$) on or near the brane. We obtain the solution using a linear approximation and generalizing Misner's method of images [19, 20] to higher dimensions. We then compute the relevant physical quantities. Lastly, we apply our variational principle (1). From this, we find a static black hole on the brane, and we determine its stability and binding energy.

A. Solution from method of images

The boundary value problem consists of (12), (18), and (19). For a small black hole sufficiently close to the brane ($|\mathbf{x}| \ll \ell$), the brane tension and cosmological constant can be neglected, so we approximate $\ell \to \infty$. This reduces (12) and (19) to an effective linear problem in an asymptotically flat space,

$$\nabla^2\psi = 0 \ , \quad \partial_z\psi\Big|_{z=0} = 0 \ , \quad \psi \underset{|\mathbf{x}|\to\infty}{\longrightarrow} 1 \ . \tag{20}$$

We implement the isometries (18) by using two symmetric throats ($j = 1, 2$) on either side of the brane ($z = 0$) and requiring inversion isometry across each throat,

$$J_j[\psi] = \psi \ , \quad \mathbf{C}_1 = -\mathbf{C}_2 = (\vec{0}, z_1) \ . \tag{21}$$

To construct the metric outside the throats, we now generalize Misner's method of images [19, 20] to higher dimensions D. The procedure is illustrated in Fig. 2.

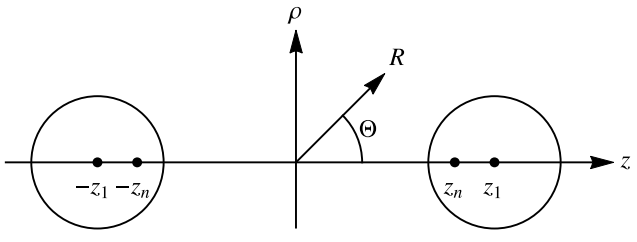

FIG. 2. The method of images. The black hole throat (right) and its orbifold mirror copy (left) are equidistant from the brane ($z = 0$). The throat coordinate radius is $a = c\,\mathrm{csch}\,\mu_0$. Image points at $\pm z_n$ and coordinates (R, Θ) are also shown.

From (13b), we first note that $J_j[1]$ is a pole at $\mathbf{C}_j$ of strength a^{D-3}, and the action of J_j on a pole (at $\mathbf{y}$ of strength q) is a pole at $J_j\mathbf{y}$ of strength

$$q' = q\,\frac{a^{D-3}}{|\mathbf{y} - \mathbf{C}_j|^{D-3}} \ . \tag{22}$$

We solve (20)–(21) by an infinite series $\psi = S[1]$, where

$$S = 1 + \sum_{n=1}^{\infty} \left[(J_1 J_2 J_1 \cdots J_{i_n}) + (J_2 J_1 J_2 \cdots J_{i'_n}) \right] \ . \tag{23}$$

We can easily verify that $J_j[S] = S$, which guarantees that ψ satisfies the inversion isometry in (21). Since each term in parentheses yields a pole,

$$\psi = 1 + \sum_{n=1}^{\infty} q_n \left(\frac{1}{|\mathbf{x} - \mathbf{x}_n|^{D-3}} + \frac{1}{|\mathbf{x} + \mathbf{x}_n|^{D-3}} \right) \ , \tag{24}$$

where the poles at $\pm\mathbf{x}_n = (\vec{0}, \pm z_n)$ lie inside the throats, and $\mathbf{x}_1 = \mathbf{C}_1$. By reflection symmetry, poles at $\pm\mathbf{x}_n$ have equal coefficients and $\partial_z\psi = 0$ at the brane. Since $\mathbf{x}_n = J_1(-\mathbf{x}_{n-1})$ we have from (13a) and (22), respectively,

$$z_n = z_1 - \frac{a^2}{z_1 + z_{n-1}} \ , \quad \frac{q_n}{q_{n-1}} = \left(\frac{a}{z_1 + z_{n-1}} \right)^{D-3} \ , \tag{25}$$

with solutions (easily proved by induction)

$$z_n = c\coth n\mu_0 \ , \quad q_n = (c\,\mathrm{csch}\, n\mu_0)^{D-3} \ . \tag{26}$$

Here $a = c\,\mathrm{csch}\,\mu_0$, where μ_0 is a dimensionless measure of the throat-brane separation, and c is a scale parameter. As in [20], bispherical coordinates (μ, η) are defined by

$$\tanh\mu = \frac{2cz}{\rho^2 + z^2 + c^2} \ , \quad \tan\eta = \frac{2c\rho}{\rho^2 + z^2 - c^2} \ . \tag{27}$$

In these coordinates, the throats are the surfaces $\mu = \pm\mu_0$, and the brane is the surface $\mu = 0$. Also, the line joining the foci $(\vec{\rho}, z) = (\vec{0}, \pm c)$ is $\eta = \pi$. In bispherical coordinates, the metric is

$$ds^2 = \Phi^{4/(D-3)} c^2 \left(d\mu^2 + d\eta^2 + \sin^2\eta\, d\omega_{D-3}^2 \right) \ , \tag{28}$$

where, with $\nu = (D-3)/2$,

$$\Phi = \sum_{n=-\infty}^{\infty} \left[\cosh(\mu + 2n\mu_0) - \cos\eta \right]^{-\nu} \ , \tag{29}$$

This can be expanded in Gegenbauer polynomials C_j^ν,

$$\Phi = \sum_{n=0}^{\infty} \sum_{j=0}^{\infty} \frac{2^{(D-1)/2}}{e^{\mu(2n+1)(j+\nu)}}\, C_j^\nu(\cos\eta) \ . \tag{30}$$

Another useful coordinate system is provided by spherical coordinates centered at $\mathbf{x} = 0$,

$$ds^2 = \psi^{4/(D-3)} \left[dR^2 + R^2 \left(d\Theta^2 + \sin^2\Theta\, d\omega_{D-3}^2 \right) \right] \ , \tag{31}$$

where for $R > z_n$ we have the multipole expansion

$$\psi = 1 + \sum_{n=1}^{\infty} \frac{2q_n}{R^{D-3}} \left[1 + \sum_{k=1}^{\infty} \left(\frac{z_n}{R} \right)^{2k} C_{2k}^\nu(\cos\Theta) \right] \ . \tag{32}$$

Also, by (27), the throat surface $R_t(\Theta)$ is the solution to

$$R_t^2 - (2c\coth\mu_0\cos\Theta) R_t + c^2 = 0 \ . \tag{33}$$

B. Physical properties and binding energy

We now compute the physical quantities needed to apply our variational principle (1) and calculate the binding energy. The throat-brane separation is

$$L = c \int_0^{\mu_0} d\mu \, [\Phi(\mu,\pi)]^{2/(D-3)} \ . \tag{34}$$

For $D = 5$, we find from (29)

$$L = c \sum_{n=-\infty}^{\infty} \left[\tanh(n+\tfrac{1}{2})\mu_0 - \tanh(n-\tfrac{1}{2})\mu_0 \right] \ . \tag{35}$$

Evaluating the sum using $\lim_{N\to\infty} \sum_{-N}^{N}$ yields simply

$$L = c \ . \tag{36}$$

From the monopole term in (32), the mass is

$$M = \frac{(D-2)\omega_{D-2}}{4\pi G_D} \sum_{n=1}^{\infty} q_n \ , \tag{37}$$

with ω_{D-2} the area of the unit $(D-2)$-sphere. One finds $L^{D-3}/(G_D M)$ is an increasing function of μ_0, so μ_0 is a dimensionless measure of the throat-brane separation, as stated earlier. For sufficiently large L, the apparent horizon is the throat, whose area A_t is

$$A_t = c^{D-2}\omega_{D-3} \int_0^{\pi} d\eta \, (\sin\eta)^{D-3} \Phi(\mu_0,\eta)^p \ , \tag{38}$$

where $p = 2(D-2)/(D-3)$. For sufficiently small L, the apparent horizon $R(\Theta)$ is the outermost extremal surface, surrounding the throat (33) and intersecting the brane. The area functional is

$$A = \omega_{D-3} \int_0^{\pi} d\Theta \ (\sin\Theta)^{D-3} R^{D-3} \sqrt{R^2 + \dot{R}^2} \, \psi^p \ , \tag{39}$$

where $\dot{R} \equiv dR/d\Theta$. Extremizing this area A gives

$$\frac{R + \ddot{R}}{1 + \dot{R}^2/R^2} = -\dot{R} \left[(D-3)\cot\Theta + p \, \frac{\partial_\Theta \psi}{\psi} \right] + R \left[(D-1) + p \, \frac{R \partial_R \psi}{\psi} \right] \ . \tag{40}$$

At $\Theta = 0$, this becomes (by L'Hôpital's rule)

$$2\ddot{R} = (D-2)R + pR^2 \frac{\partial_R \psi}{\psi} \ . \tag{41}$$

To find extremal surfaces surrounding the throat, we numerically integrate (40), with the initial conditions $R(0) > R_t(0)$ and $\dot{R} = 0$. If $\dot{R} = 0$ at $\Theta = \pi/2$, then $R(\Theta)$ is one of two extremal surfaces, as also occurs in Brill-Lindquist initial data [23]. The outermost extremal surface is the apparent horizon, with area A_o given by (39). We numerically find that such extremal surfaces surround the throat for $\mu_0 \le \bar{\mu}_0$, where $\bar{\mu}_0 \simeq 1.36$, 0.75, 0.51 for $D = 4$, 5, 6, respectively.

To apply our variational principle (1), we extremize the mass M while holding the apparent horizon area A constant. Since c is a scale parameter, $A = c^{D-2}\hat{a}$, where $\hat{a}$ is dimensionless. For a constant value A, we thus set

$$c(\mu_0) = \left[\frac{A}{\hat{a}(\mu_0)} \right]^{1/(D-2)} \ , \quad \hat{a} = \begin{cases} \hat{a}_o & \text{if } \mu_0 < \bar{\mu}_0 \\ \hat{a}_t & \text{if } \mu_0 > \bar{\mu}_0 \end{cases} \tag{42}$$

Here $\hat{a}_o$ is found numerically as described above, and

$$\hat{a}_t(\mu_0) = \omega_{D-3} \int_0^{\pi} d\eta \, (\sin\eta)^{D-3} \Phi(\mu_0,\eta)^p \ . \tag{43}$$

The mass M at fixed area is then given by (37), using c in (42) to evaluate the coefficients q_n in (26). For $D = 5$, we have $L = c(\mu_0)$ by (36). For large throat-brane separation ($\mu_0 \gg 1$),

$$\frac{G_5 M}{6\pi c^2} \simeq e^{-2\mu_0} + 3e^{-4\mu_0} \ , \quad \frac{\hat{a}_t}{128\pi^2} \simeq e^{-3\mu_0} + 6e^{-5\mu_0} \ . \tag{44}$$

Combining these gives, for large throat-brane separation,

$$M \simeq M_A - \frac{G_5 M_A^2}{6\pi L^2} \ . \tag{45}$$

This has the physically expected form: the first term is the rest mass (2), and the second term is the interaction energy of the black hole with its orbifold image.

The mass M as a function of L at fixed apparent horizon area is plotted in Fig. 3 for $D = 5$. By our variational principle (1), the extremum at $L \to 0$ is a static black hole. This black hole on the brane is well known numerically [12]. Our results show that this black hole is a local mass minimum, which indicates it is stable against translations transverse to the brane.

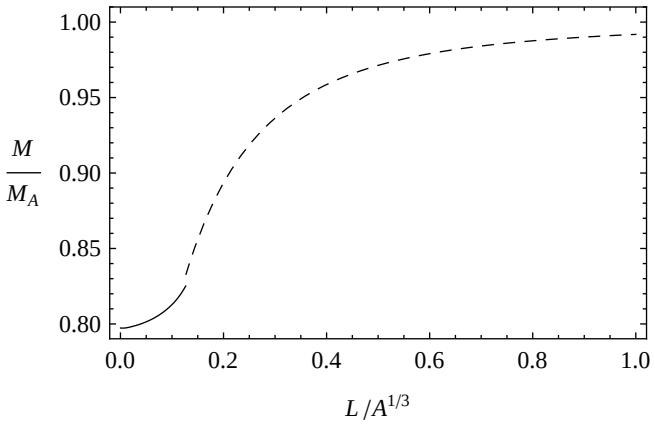

FIG. 3. Mass M at fixed area A, for $D = 5$. Solid line: the black hole is on the brane (A is the area of the outermost extremal surface). Dashed line: the black hole is off the brane (A is the throat area).

The black hole's stability is also indicated by its large binding energy. At $L \to 0$, the value $M \to M_1$ in Fig. 3 is

the value (6) we found previously in deriving our binding energy result (7). For $\mathbb{Z}_2$ orbifold symmetry, this value is $M_1 = 2^{-1/3} M_A \simeq 0.79 M_A$, where the mass far from the brane is $M_2 \simeq M_A$ by (45). From our binding energy result (7), the minimum binding energy is

$$E_B = \left(2^{1/3} - 1\right) M_1 \ . \tag{46}$$

This binding energy is of order M_1, and hence substantial. Since brane tension and cosmological constant have been neglected here, this result explicitly demonstrates the significant role of the orbifold symmetry in binding the black hole to the brane, as discussed in section II.

VI. BLACK HOLES FAR FROM THE BRANE

In this section, we solve the boundary value problem of section IV, for a small black hole ($a \ll \ell$, $a \ll z_1$) farther from the brane than in section V. The setup is illustrated in Fig. 4. For $D = 5$, we will first construct the asymptotically RS2 solution for ψ using a field expansion,

$$\psi = \psi_0 + \psi_0^2 \, \phi_1 + \psi_0^2 \sum_{i \geq 2} \phi_i \ . \tag{47}$$

The field ϕ_1 provides all of our physical results. After computing the relevant physical quantities, we then apply our variational principle (1) to find a static black hole off the brane. We also find small corrections to the binding energy (46). Lastly, we examine the perturbations ϕ_i ($i \geq 2$) to ensure that the expansion (47) is well controlled.

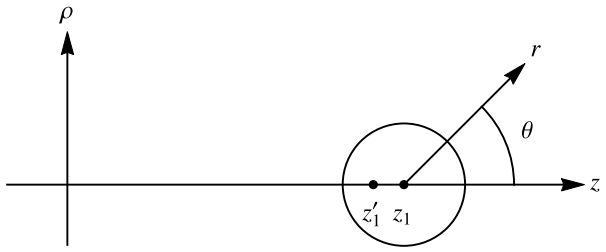

FIG. 4. A black hole farther from the brane than in section V. The coordinates (ρ, z) and (r, θ) are the same as in Fig. 1. The source point at z_1' is used in the solution for the field ϕ_1.

A. Perturbation series

The boundary value problem for the field ψ consists of (12), (18), and (19). To solve this, we define a related field ϕ and two operators $(\mathcal{H}, \mathcal{D})$ by

$$\begin{aligned} \psi &= \psi_0 + \psi_0^2 \phi \\ \mathcal{H} f &= \psi_0^2 \left(\nabla^2 - \frac{4\psi_0}{\ell} \, \partial_z \right) f \\ \mathcal{D} f &= - \left[r \partial_r + \frac{\ell + z_1 - r\cos\theta}{\ell + z_1 + r\cos\theta} \right] f \ . \end{aligned} \tag{48}$$

The constraint (12) is then

$$\mathcal{H}\phi = \frac{2}{\ell^2} \psi_0^5 \left(3\phi^2 + \psi_0 \phi^3 \right) \tag{49}$$

and the boundary conditions (19) are

$$\left(\partial_z \phi + \frac{\phi^2}{\ell} \right) \Big|_{z=0} = 0 \ , \quad \mathcal{D}\phi \Big|_{r=a} = \frac{1}{\psi_0(z_1)} \ , \quad \phi \underset{|\mathbf{x}| \to \infty}{\longrightarrow} 0 \ . \tag{50}$$

We now write ϕ as a perturbation series,

$$\phi = \phi_1 + \sum_{i \geq 2} \phi_i \ . \tag{51}$$

All of our physical results will be due to the primary field ϕ_1. The fields ϕ_i with $i \geq 2$ are perturbations. We substitute (51) into (49)–(50), and collect terms of order i. We also introduce parameters α_i for the throat boundary condition, obeying $\sum_i \alpha_i = 1$, and we let $a A_i = \alpha_i / \psi_0(z_1)$. This results in the following boundary value problem to solve at each order i,

$$\mathcal{H}\phi_i = F_i \ , \quad \partial_z \phi_i \Big|_{z=0} = -B_i \Big|_{z=0} \ , \quad \mathcal{D}\phi_i \Big|_{r=a} = a A_i \tag{52}$$

and $\phi_i \to 0$ as $|\mathbf{x}| \to \infty$. The sources F_i and B_i involve only fields ϕ_j with $j < i$. For the primary field ϕ_1,

$$F_1 = 0 \ , \quad B_1 = 0 \ . \tag{53}$$

At second order,

$$F_2 = \frac{6}{\ell^2} \psi_0^5 \phi_1^2 \ , \quad B_2 = \frac{1}{\ell} \psi_0^2 \phi_1^2 \ . \tag{54}$$

At third order,

$$F_3 = \frac{2}{\ell^2} \psi_0^5 \left(\psi_0 \phi_1^3 + 6 \phi_1 \phi_2 \right) \ , \quad B_3 = \frac{2}{\ell} \psi_0^2 \phi_1 \phi_2 \ , \tag{55}$$

and this process continues to higher orders.

B. Green function $\mathcal{G}_N$ and primary field ϕ_1

For the operator $\mathcal{H}$, the Neumann Green function $\mathcal{G}_N$ can be regarded as the field of a point source, defined by

$$\mathcal{H}\mathcal{G}_N(\mathbf{x}, \mathbf{x}') = -\delta(\mathbf{x} - \mathbf{x}') \ , \quad \partial_z \mathcal{G}_N \Big|_{z=0} = 0 \ . \tag{56}$$

$\mathcal{G}_N$ vanishes as $|\mathbf{x}| \to \infty$, with no throat boundary condition. This can be solved with a Fourier method: we set $\delta(\mathbf{x} - \mathbf{x}') = \delta(\vec{\rho} - \vec{\rho}\,') \delta(z - z')$ and

$$\delta(\vec{\rho} - \vec{\rho}\,') = \frac{1}{(2\pi)^3} \int_{-\infty}^{\infty} d^3k \, e^{i\vec{k} \cdot (\vec{\rho} - \vec{\rho}\,')} \ , \tag{57a}$$

$$\mathcal{G}_N(\mathbf{x}, \mathbf{x}') = \frac{1}{(2\pi)^3} \int_{-\infty}^{\infty} d^3k \, e^{i\vec{k} \cdot (\vec{\rho} - \vec{\rho}\,')} F \ , \tag{57b}$$

where $F(\vec{k}, z, z')$ is to be determined. Substituting (57) into (56) yields a differential equation for F, whose solution involves modified Bessel functions, $I_{5/2}$ and $K_{5/2}$. Performing the integral (57b) then yields the result

$$4\pi^2 \mathcal{G}_N(\mathbf{x}, \mathbf{x}') = \frac{\psi_0(z)^{-2}}{|\mathbf{x} - \mathbf{x}'|^2} + \frac{\psi_0(z)^{-2}}{|\mathbf{x} - \widetilde{\mathbf{x}}'|^2} + c_1 \ln \frac{|\mathbf{x} - \mathbf{x}'|}{|\mathbf{x} - \widetilde{\mathbf{x}}'|} + \psi_0(z')^2 \mathcal{J} \ . \quad (58)$$

The first two terms are expected: a source at $\mathbf{x}' = (\vec{\rho}', z')$ and a source at the orbifold image point $\widetilde{\mathbf{x}}' = (\vec{\rho}', -z')$. The additional terms are

$$\mathcal{J} = \frac{6 \tan^{-1}[R/(z+z')]}{\ell R} + \frac{3zz'}{\ell^4} + c_2 \, \mathrm{Re}\left[ie^{\xi}\Gamma(0,\xi)\right] \quad (59)$$

where

$$R = |\vec{\rho} - \vec{\rho}'| \ , \quad \xi = (z + z' + iR)/\ell \quad (60)$$

and

$$c_1 = \psi_0(z')^2 \frac{3}{2\ell^4}\left[R^2 + (\ell+z)^2 + (\ell+z')^2\right] \ ,$$
$$c_2 = -\frac{2}{\ell^5 R}(\ell^2 - \ell z + z^2)(\ell^2 - \ell z' + z'^2) \ . \quad (61)$$

For $\mathbf{x}$ near $\mathbf{x}'$, the first term in (58) dominates, giving the $1/|\mathbf{x}-\mathbf{x}'|^2$ behavior of 5-dimensional gravity. At large R, the first term in (59) dominates, giving the $1/R$ behavior of 4-dimensional gravity, which is the RS2 phenomenon of localized gravity. At large R and large z, respectively,

$$\mathcal{G}_N \simeq \frac{3\psi_0(z')^2}{4\pi\ell R} \ , \quad \mathcal{G}_N \simeq \frac{4\psi_0(z')^2}{\pi^2 \ell z} \ . \quad (62)$$

We may construct the field ϕ_1 from $\mathcal{G}_N$ by taking $\mathbf{x}'$ inside the throat and forming a multipole expansion

$$\phi_1(\mathbf{x}) = \sum_{n=0}^{\infty} f_n \left(\partial_{z'}\right)^n \mathcal{G}_N(\mathbf{x}, \mathbf{x}')\Big|_{\mathbf{x}'=\mathbf{x}'_1} \ . \quad (63)$$

We approximate this sum as an off-center point source,

$$\phi_1 \simeq f_0 \, \mathcal{G}_N(\mathbf{x}, \mathbf{x}'_1) \ , \quad \mathbf{x}'_1 = (\vec{0}, z'_1) \ , \quad z'_1 = z_1 - d \ . \quad (64)$$

We determine f_0 and d by the throat boundary condition. For $z_1 \ll \ell$, we use the first two terms in (58) with

$$\phi_1 \simeq \frac{f_0}{4\pi^2\psi_0^2} \sum_{k=0}^{1} \frac{C_k^1(\cos\theta)}{(-1)^k}\left[\frac{d^k}{r^{2+k}} + \frac{r^k}{w^{2+k}}\right] \ , \quad (65)$$

where $\psi_0 = \ell/(\ell + z_1 + r\cos\theta)$ and $w = 2z_1 - d \simeq 2z_1$. For $z_1 \gg \ell$, it suffices to use the first and third terms in (58), with

$$\phi_1 \simeq \frac{f_0}{4\pi^2\psi_0^2} \sum_{k=0}^{1} \frac{C_k^1(\cos\theta)}{(-1)^k} \frac{d^k}{r^{2+k}} + \frac{3f_0}{4\pi^2\ell^2}\left(1 + \frac{r\cos\theta + d}{\ell + z_1}\right)\ln\left(\frac{r}{2z_1}\right) \ . \quad (66)$$

Linearizing the throat boundary condition in $\cos\theta$ gives

$$f_0 \simeq \alpha_1 4\pi^2 a^2 \psi_0(z_1)\,(1+\varepsilon) \ . \quad (67)$$

For $z_1 \ll \ell$, we find

$$\varepsilon = \left(\frac{a}{2z_1}\right)^2 \ , \quad d \simeq a\,\psi_0(z_1)\left(\frac{a}{2\ell} + \frac{a^3}{8z_1^3}\right) \ . \quad (68)$$

For $z_1 \gg \ell$, we find

$$\varepsilon = 3\left[\psi_0(z_1)\frac{a}{\ell}\right]^2 \ln\left(\frac{a}{2z_1}\right) \ , \quad d \simeq \frac{a^2\psi_0(z_1)}{2\ell}\left(1 - \frac{\varepsilon}{2}\right) \ . \quad (69)$$

C. Physical properties and binding energy

We now compute the physical quantities needed to apply our variational principle (1) and calculate the binding energy. The relevant quantities are the throat-brane separation L, the throat area A, and the mass M. In this section, we are neglecting the perturbation fields ϕ_i ($i \geq 2$), so $\alpha_1 = 1$ is the only throat boundary condition parameter needed here. The throat-brane separation is

$$L = \int_0^{z_1 - a} dz\,\psi \simeq \int_0^{z_1} dz\,\psi_0(z) = -\ell \ln\left[\psi_0(z_1)\right] \ . \quad (70)$$

We now evaluate the throat area A. Near the throat,

$$\psi \simeq \psi_0(z_1) + \frac{f_0}{4\pi^2 a^2}(1+\varepsilon) \simeq 2\psi_0(z_1)(1+\varepsilon) \ . \quad (71)$$

This gives the throat area $A = 2\pi^2 a^3 \psi^3$. It will be convenient to use the related rest mass M_A, which by (2) is given by $G_5 M_A = (3\pi/8)a^2\psi^2$. Solving this for a gives

$$a^2 \simeq \frac{2G_5 M_A}{3\pi\psi_0(z_1)^2}\,(1 - \varepsilon') \ , \quad (72)$$

where for $z_1 \ll \ell$ and $z_1 \gg \ell$, respectively,

$$\varepsilon' = \frac{G_5 M_A}{3\pi z_1^2 \psi_0(z_1)^2} \ , \quad \varepsilon' = \frac{2G_5 M_A}{\pi\ell^2} \ln\left[\frac{G_5 M_A}{6\pi z_1^2 \psi_0(z_1)^2}\right] \ . \quad (73)$$

We defined the mass M for an asymptotically RS geometry in [17], which for the large ρ asymptotics (62) yields

$$M = \frac{3}{8\pi G_5}\psi_0(z'_1)^2 f_0 \ . \quad (74)$$

Using (67) and (72), this can be rewritten as

$$M \simeq \psi_0(z_1) M_A - \psi_0(z_1) M_A \frac{\varepsilon'}{2} \ . \quad (75)$$

The first term is the redshifted rest mass, and the second term is the interaction energy of the black hole with its orbifold image. The redshift factor $\psi_0(z_1)$ indicates the repelling gravitational field of the positive-tension brane.

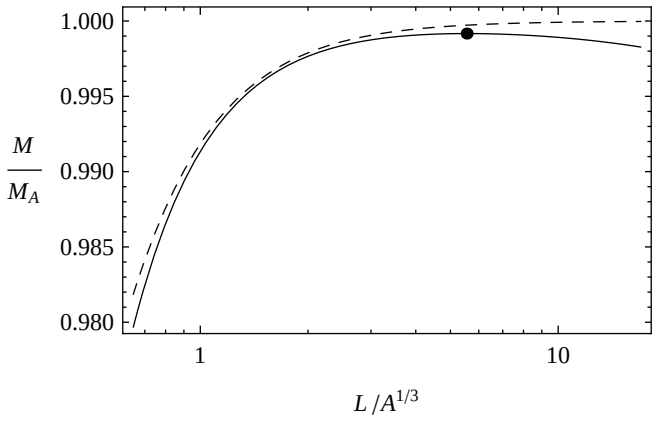

FIG. 5. Solid line: Mass M at fixed throat area $A = 10^{-12}\ell^3$. The dot denotes the mass extremum. Dashed line: the asymptotically flat approximation of Fig. 3.

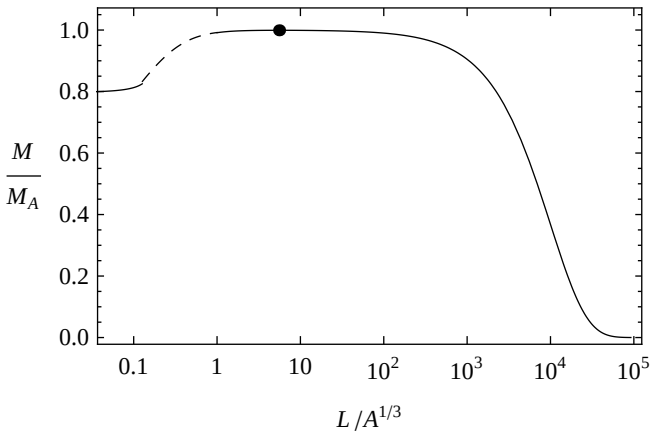

FIG. 6. Combination of Fig. 3 and Fig. 5. Leftmost solid line: the black hole is on the brane. Dashed line: the black hole is off the brane (asymptotically flat approximation). The dot denotes the mass extremum of Fig. 5. Rightmost solid line: extension of the RS2 mass function of Fig. 5.

In Fig. 5, we plot the mass M at fixed area A. It agrees well with the asymptotically flat approximation of Fig. 3 in the regime where the Newtonian form (45) is valid. There is a mass extremum (represented by the dot in Fig. 5), where the black hole's repulsion from the brane is balanced by its attraction to its orbifold image. Taking $z_1 \ll \ell$ in (75) gives

$$M \simeq M_A \left(1 - \frac{z_1}{\ell}\right) - \frac{G_5 M_A^2}{6\pi z_1^2} \ . \tag{76}$$

At fixed M_A and ℓ, the mass extremum ($dM/dz_1 = 0$) occurs at the location z_1 given by

$$(z_1)_{\rm ext} = \left(\frac{G_5 M_A \ell}{3\pi}\right)^{1/3} \quad , \quad L_{\rm ext} \simeq (z_1)_{\rm ext} \ . \tag{77}$$

By our variational principle (1), this mass extremum represents a static black hole. It is a local maximum, hence this black hole is unstable against translations transverse to the brane. The binding energy $E_B = M_{\rm ext} - M_1$ of a small black hole on the brane is

$$E_B \simeq \left[2^{1/3} - 1 - \frac{3}{2}\left(\frac{2G_5 M_A}{3\pi\ell^2}\right)^{1/3}\right] M_1 \ . \tag{78}$$

This is smaller than our previous estimate (46), consistent with the brane's repelling gravitational field. For large separation L from the brane, the brane's repulsion dominates, and the mass at fixed area is $M \simeq e^{-L/\ell} M_A$, as shown in Fig. 6.

D. Perturbations

As indicated earlier, the perturbations ϕ_i ($i \geq 2$) are not needed for our main physical results, but we consider them here to ensure that our field expansion for ϕ is well controlled. The perturbations ϕ_i ($i \geq 2$) may be found by first constructing a new Green function $\mathcal{G}$ that satisfies the same relations (56) as the Neumann Green function $\mathcal{G}_N$, and additionally $\mathcal{D}\mathcal{G} = 0$ at the throat. We take $\mathcal{G}(\mathbf{x}, \mathbf{x}') = \mathcal{G}_N(\mathbf{x}, \mathbf{x}') + \mathcal{F}_N(\mathbf{x}, \mathbf{x}')$ where

$$\mathcal{F}_N(\mathbf{x}, \mathbf{x}') = \sum_{n=0}^{\infty} \sum_{m=1}^{(n+1)^2} f_{nm} \Gamma_{nm} \ , \tag{79}$$

and

$$\Gamma_{nm} = \mathcal{D}_{nm} \mathcal{G}_N(\mathbf{x}, \mathbf{v})\Big|_{\mathbf{v}=\mathbf{v}_0} \ ,$$
$$\mathcal{D}_{nm} = \sum_{i,j,k,l} S^{ijk}_{nm}\, \partial^i_{v_1} \partial^j_{v_2} \partial^k_{v_3} \partial^l_{v_4} \ . \tag{80}$$

Here $\mathbf{v}$ lies inside the throat, so $\mathcal{H}\mathcal{F}_N = 0$. The quantities S^{ijkl}_{nm} are constants and $\mathcal{D}_{nm}$ is the order n derivative operator that generates the spherical harmonics Y_{nm},

$$\mathcal{D}_{nm} \left(\frac{1}{4\pi^2 |\mathbf{x} - \mathbf{v}|^2}\right)\Big|_{\mathbf{v}=\mathbf{v}_0} = \frac{Y_{nm}}{|\mathbf{x} - \mathbf{v}_0|^{n+2}} \ . \tag{81}$$

Here $1 \leq m \leq (n+1)^2$ which motivates the sum in (79). Letting $\mathbf{v}_0$ denote the throat center, it follows that

$$a^{n+2} \psi_0^2 \Gamma_{nm}\Big|_{r=a} = \sum_{n',m'} (\delta_{nmn'm'} + \Delta_{nmn'm'}) Y_{n'm'} \tag{82}$$

with $\Delta_{nmn'm'}$ small quantities. This equation should be invertible, so Γ_{nm} are a complete set of functions on the throat, and the coefficients f_{nm} can be determined by the throat boundary condition.

The formal solution to (52) for the perturbation ϕ_i is then

$$\psi_0(z)^2 \phi_i(\mathbf{x}) = -\int d^4\bar{x}\, \sqrt{h}\, \mathcal{G}\, \psi_0^2 F_i + \int d^3\bar{x}\, \sqrt{\bar{\sigma}}\, \mathcal{G}\, \psi_0^4 B_i + \int d^3\bar{x}\, \sqrt{\bar{\sigma}}\, \mathcal{G}\, \psi_0^4 A_i \ . \tag{83}$$

In these integrals, $\bar{h}$ and $\bar{\sigma}$ denote flat metrics, and only $\mathcal{G}(\bar{\mathbf{x}}, \mathbf{x})$ depends on $\mathbf{x}$. At large $\bar{\rho}$, the bulk and brane sources $(F_i,\ B_i)$ contain terms which fall off as $1/\bar{\rho}^2$ or $1/\bar{\rho}^3$. In (83), terms with $1/\bar{\rho}^2$ falloff produce divergent bulk and brane integrals, and terms with $1/\bar{\rho}^3$ falloff produce divergent contributions to the mass M. However, these are only apparent divergences, not true divergences, since we can reformulate the perturbations so that no divergences occur, by setting $\phi_i = \widetilde{\phi}_i + \Phi_i$ with Φ_i a suitably chosen regulator. The regulated perturbation $\widetilde{\phi}_i$ is then

$$\psi_0(z)^2 \widetilde{\phi}_i(\mathbf{x}) = -\int d^4\bar{x}\,\sqrt{\bar{h}}\,\mathcal{G}\,\psi_0^2 \widetilde{F}_i + \int d^3\bar{x}\,\sqrt{\bar{\sigma}}\,\mathcal{G}\,\psi_0^4 \widetilde{B}_i + \int d^3\bar{x}\,\sqrt{\bar{\sigma}}\,\mathcal{G}\,\psi_0^4 \widetilde{A}_i\ , \tag{84}$$

where the regulated sources are

$$\widetilde{F}_i = F_i - \mathcal{H}\Phi_i\ , \quad \widetilde{B}_i = B_i + \partial_z \Phi_i\ , \quad a\widetilde{A}_i = aA_i - \mathcal{D}\Phi_i \tag{85}$$

and each regulator Φ_i must ensure the large ρ falloff of $\widetilde{F}_i$ and $\widetilde{B}_i$ is $1/\rho^n$ where $n \geq 4$. Suitable examples are

$$\Phi_2 = \psi_0(z) \frac{(2G_5 m_1)^2}{\ell^2(\rho^2 + b_1^2)}\ ,$$
$$\Phi_3 = \psi_0(z) \frac{8G_5^2 m_1 m_2}{\ell^2(\rho^2 + b_2^2)} + \psi_0(z)^2 \frac{(2G_5 m_1)^3}{\ell^3(\rho^3 + b_3^3)}\ , \tag{86}$$

with b_j constants. Here m_i is the mass contribution at order i to the total mass $M = \sum_i m_i$. One can continue choosing regulators at higher orders, although no regulators are needed at fourth order or higher, if one tunes $m_i = 0$ at second order and higher, which can be achieved by tuning the throat boundary condition parameters α_i.

VII. BOUNDS FOR SMALL BLACK HOLES AND RELATED PHENOMENOLOGY

Below, we will obtain upper bounds, $M \lesssim M_*$ and $A \lesssim A_*$, for the black hole mass M and area A, for which our results of sections V and VI for small black holes in RS2 are expected to be valid. We consider black holes on the brane and off the brane, respectively, in sections VII A and VII B. In each case, we relate our bounds to phenomenology, including an application in section VII C to RS1 and searches for small black holes produced at colliders. We denote the reduced Planck masses in five and four dimensions as $M_5 = (8\pi G_5)^{-1/3}$ and $M_{Pl} = (8\pi G_4)^{-1/2} = 2.4 \times 10^{18}$ GeV in standard units.

A. Small black holes on the brane in RS2

In RS2, we first obtain upper bounds $(M_*,\ A_*)$ on black hole mass and area, and then consider the related phenomenology. A small black hole on the brane is nearly spherical, with bulk area A and mass M related by (5),

$$A = 2^{1/(D-3)}\, c_D\, (G_D M)^{(D-2)/(D-3)}\ . \tag{87}$$

Here and below, the numerical coefficients c_n are

$$c_n = \left[\frac{1}{\omega_{n-2}} \left(\frac{16\pi}{n-2}\right)^{n-2}\right]^{1/(n-3)}\ , \tag{88}$$

with ω_{n-2} the area of the $(n-2)$-dimensional unit sphere. The small black hole behavior (87) ceases to be valid at mass and length scales that can be estimated from the properties of larger black holes, which we now consider.

In RS2, a very large static black hole on the brane has a flattened (pancake) shape [15, 24], for which the area A in the bulk and circumference $\mathcal{B}$ on the brane are [15]

$$A = \frac{\ell\,\mathcal{B}}{D-3}\ , \quad \mathcal{B} = c_{D-1}\,(G_{D-1}M)^{(D-3)/(D-4)}\ . \tag{89}$$

On the brane, $\mathcal{B}$ is a $(D-3)$-dimensional area and the Newton gravitational constant is $G_{D-1} = (D-3)G_D/\ell$. Combining this with (89) shows that a large black hole on the brane has bulk area A and mass M related by

$$A = c_{D-1}(D-3)^{1/(D-4)} \left[\frac{(G_D M)^{D-3}}{\ell}\right]^{1/(D-4)}\ . \tag{90}$$

We now find an upper bound on the mass M_* and area A_* for which the small black hole relation (87) is valid, by equating the two areas in (87) and (90). These intersect at the value M_* determined by the AdS length ℓ,

$$G_D M_* = \frac{2^{D-4}}{(D-3)^{D-3}} \left(\frac{c_D}{c_{D-1}}\right)^{(D-3)(D-4)} \ell^{D-3}\ , \tag{91}$$

with A_* given by (87) with $M = M_*$. The result (91) shows that a black hole with $M \lesssim M_*$ is small compared to the AdS curvature length scale, $G_D M \ll \ell^{D-3}$. This is illustrated in Fig. 7 for $D = 5$, for which $G_5 M_* = (4/27)\ell^2 \simeq 0.05\,\ell^2$ and $A_* \simeq 0.2\,\ell^3$.

The bound $M \lesssim M_*$ is consistent with the assumption $a \ll \ell$ on the throat coordinate radius a used in this paper. To see this, recall from section V that for small throat-brane separation ($\mu_0 \ll 1$), the black hole apparent horizon is the outermost extremal surface. As $\mu_0 \to 0$, this surface is a sphere, $R = R_0$, which can be found analytically by taking $R \gg z_n$ in (32), for which the monopole term in ψ dominates. Solving (40) yields

$$R_0^{D-3} = 2\sum_{n=1}^{\infty} q_n = 2\,\zeta(D-3)\,a^{D-3}\ , \tag{92}$$

where ζ is the Riemann zeta function. The last equality in (92) follows from using q_n in (26) with $c = a/\mathrm{csch}\,\mu_0$ and $(\mathrm{csch}\,n\mu_0)/(\mathrm{csch}\,\mu_0) = 1/n + O(\mu_0^2)$ as $\mu_0 \to 0$. The resulting area A of the surface $R = R_0$ is

$$A = \frac{1}{2}\,[8\,\zeta(D-3)]^{(D-2)/(D-3)}\,\omega_{D-2} a^{D-2}\ . \tag{93}$$

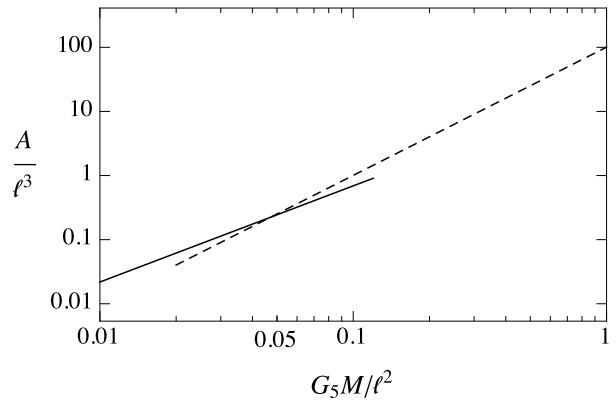

FIG. 7. Relation between area A and mass M for asymptotically RS2 black holes on the brane, in $D = 5$, for small black holes (solid line, $M \lesssim M_*$) and large black holes (dashed line). These intersect at $G_5 M_* \simeq 0.05\,\ell^2$. Each axis is logarithmic.

The corresponding upper bound $a \lesssim a_*$ on the radius a is given by using the area A_* in (93). For $D = 5$, the value $A_* \simeq 0.2\,\ell^3$ found above and $\zeta(2) = \pi^2/6$ gives $a_* \simeq 0.08\,\ell$. This is an upper bound on a for the validity of the condition $a \ll \ell$ used in section V.

The phenomenology of the RS2 model is currently based on experiments that probe corrections to the inverse square law of Newtonian gravity. If our observed universe is indeed a brane in the RS2 model, torsion pendulum experiments [25] yield the bound $\ell < 0.014$ mm on the AdS curvature length ℓ. The AdS length ℓ relates the effective Planck masses in five and four dimensions in RS2 by [2] $M_5 = (8\pi M_{Pl}^2/\ell)^{1/3}$, which for $\ell < 0.014$ mm yields the lower bound $M_5 > 1.3 \times 10^6$ TeV. This energy scale, which is relevant for the production of small black holes in particle collisions on the brane, is beyond the reach of current particle colliders, although it was suggested in [26] that high energy signatures of RS2 might be accessible by ultra high energy cosmic rays. Some progress was made in this direction in [26], by mapping out the different forms of the cross section for producing small black holes in high energy scattering experiments on the brane, for different ranges of the center of mass energy and impact parameter, compared to scales set by ℓ and M_{Pl}. Since the high energy collider phenomenology of the RS1 model is much more developed than that of RS2, in section VII C below, we will consider the phenomenology of RS1 and the energy range for which our general binding energy result (7) is applicable.

B. Small black holes off the brane in RS2

The phenomenology of RS2, relevant for black holes on the brane, has already been discussed in section VII A above. Here we obtain upper bounds (M_*, A_*) on the mass and area of small black holes localized off the brane in RS2. We will use the results of this section when we consider the RS1 model in section VII C below.

Since a small black hole is nearly spherical, the relation between its one-dimensional circumference $\mathcal{C}$ and surface area A is well approximated by

$$\mathcal{C} = 2\pi \left(\frac{A}{\omega_{D-2}} \right)^{1/(D-2)} . \qquad (94)$$

As found in (70), the black hole is located a proper distance L and coordinate distance z_1 from the brane, where

$$L \simeq -\ell \ln[\psi_0(z_1)] , \quad \psi_0(z_1) = \frac{\ell}{\ell + z_1} \simeq e^{-L/\ell} . \qquad (95)$$

Note that L essentially interpolates between the smaller of z_1 and ℓ. That is, for $z_1 \ll \ell$, we have $L \simeq z_1$, while for $\ell \ll z_1$, we have $L \simeq \ell \ln(z_1/\ell)$, which is nearly of order ℓ since the logarithm is a slowly varying function of z_1.

The condition that the black hole is small and localized off the brane can be stated geometrically as $\mathcal{C} \ll L$, hence $\mathcal{C} \lesssim L$ provides an upper bound on $\mathcal{C}$ for this small black hole regime to be valid. Expressing this in terms of the area A using (94) then yields the condition $A \lesssim A_*$, where the upper bound on the black hole area is

$$A_* = \omega_{D-2} \left(\frac{L}{2\pi} \right)^{D-2} . \qquad (96)$$

For $D = 5$, this upper bound is $A_* = L^3/(4\pi) \simeq 0.08 L^3$. The corresponding upper bound on the mass, $M \lesssim M_*$, follows from evaluating $M \simeq e^{-L/\ell} M_A$ given in (75),

$$G_5 M_* = e^{-L/\ell} \left[\frac{3\pi}{8} \left(\frac{A_*}{2\pi^2} \right)^{2/3} \right] \simeq 0.03\, e^{-L/\ell} L^2 . \qquad (97)$$

The corresponding upper bound $a \lesssim a_*$ on the radius a follows from evaluating (72) with $M_A \simeq M_* e^{L/\ell}$,

$$a_* = \frac{e^{L/\ell} L}{4\pi} \simeq 0.08\, e^{L/\ell} L . \qquad (98)$$

With L given by (95), the condition $a \lesssim a_*$ thus specifies a region in the space of parameters (a, z_1, ℓ). For the cases $z_1 \ll \ell$ and $\ell \ll z_1$, we have respectively, $a_* \simeq 0.08\, z_1$ and $a_* \simeq 0.08\, z_1 \ln(z_1/\ell)$. These are upper bounds on a for which the approach of section VI is expected to be reliable for describing an initially static small black hole localized off the brane.

C. Small black holes on the brane in RS1

Although the RS2 model is the main focus of this paper, we here discuss an application to the RS1 model, which is relevant for the possible production of small black holes in LHC experiments. Our general binding energy result (7) indicates there is substantial binding of a small black hole to a brane with orbifold symmetry.

We here obtain an upper bound on the mass for which this strong binding result can be expected to apply in the RS1 model.

In the RS1 model (see section III), our universe resides on a negative-tension brane at a proper distance L from the positive-tension brane. An upper bound on the mass, $M \lesssim M_*$, for a black hole on the negative-tension brane to be treated as small can be obtained directly from our previous result (97) in the RS2 model,

$$G_5 M_* = \left(\frac{3}{64\pi}\right) e^{-L/\ell} L^2 \simeq 0.015\, e^{-L/\ell} L^2 \ . \qquad (99)$$

This value is reduced by a factor of 2 compared to (97), since the black hole resides on the brane, and we are measuring mass on the orbifold region between the branes.

In the RS1 model [1], the higher-dimensional Newton constant is $G_5 \simeq \ell/(8\pi M_{Pl}^2)$. The RS1 model [1] can solve the hierarchy problem if $L \simeq 12\pi\ell$, for which (99) yields

$$M_* = 54\pi^2 e^{-12\pi} M_{Pl}^2 \ell \ . \qquad (100)$$

If our observed universe resides on the negative-tension brane in the RS1 model, the current phenomenological constraints on the AdS length ℓ are [4]

$$10 < M_{Pl}\ell < 100 \ , \qquad (101)$$

with $M_{Pl}\ell$ a dimensionless quantity in the standard units used here. The lower bound in (101) is due to perturbativity requirements, and the upper bound is set by high precision electroweak data. Combining (100) and (101) yields

$$5.4 \times 10^2 \text{ TeV} < M_* < 5.4 \times 10^3 \text{ TeV} \ . \qquad (102)$$

Similar bounds to (102) were found in [27] by considering ranges of coordinates, instead of the geometric quantities we examined above. We thus estimate that a black hole with mass $M \lesssim 5.4 \times (10^2 - 10^3)$ TeV may be reliably treated as small, with a corresponding large orbifold binding to the negative-tension brane as derived in this paper. For a black hole produced in a collider experiment on the brane, the black hole mass is at least of order the higher-dimensional Planck mass. The precise value of the black hole mass depends on how much energy is trapped inside the Schwarzschild radius associated with the center of mass energy. Recent LHC collider searches [5] at center of mass energy 8 TeV exclude evidence for the production of black holes with masses below 4.7–5.5 TeV, for a higher-dimensional Planck energy in the range 2–4 TeV in the RS1 model. These experimental results are consistent with our mass bound (102), which can be applied to future experimental searches for black hole production at higher center of mass energies in the TeV range or higher.

VIII. DISCUSSION

In this paper, we applied our variational principle [22] to initial data for small asymptotically RS2 black holes, and found two static black holes. We showed that the well known static black hole on the brane is stable against translations transverse to the brane, and has a large binding energy to the brane due to the brane's orbifold symmetry. This is an explicit example of a simple but general binding energy formula, given in (7), which can be used in other orbifold-symmetric braneworld models. We also found a new static black hole off the brane, at the unique location in the bulk where the black hole's repulsion from the brane is balanced by its attraction to its orbifold image, with a novel instability to transverse translations. Although the static black hole on the brane is classically stable, it would be interesting to consider its quantum tunneling through the barrier illustrated in Fig. 6. It would also be interesting to study the existence and properties of these classical solutions at larger black hole mass; numerical methods would probably be necessary.

Our results show that a small black hole produced on an orbifold-symmetric brane in RS2 is stable against leaving the brane, and we have indicated how this conclusion can be applied to models other than RS2, as long as the brane has an orbifold symmetry. On such a brane, small black holes produced in high energy experiments could be studied directly (instead of leaving behind a signature of missing energy), which is an important result for future collider experiments.

ACKNOWLEDGMENTS

We thank J. Polchinski for useful discussions. This research was supported in part by the National Science Foundation under Grant No. NSF PHY11-25915.

[1] L. Randall and R. Sundrum, Phys. Rev. Lett. **83**, 3370 (1999), arXiv:hep-ph/9905221.
[2] L. Randall and R. Sundrum, Phys. Rev. Lett. **83**, 4690 (1999), arXiv:hep-th/9906064.
[3] T. Banks and W. Fischler, (1999), arXiv:hep-th/9906038; S. B. Giddings and S. D. Thomas, Phys. Rev. **D65**, 056010 (2002), arXiv:hep-ph/0106219.
[4] S. Chatrchyan *et al.* (CMS Collaboration), Phys. Rev. Lett. **108**, 111801 (2012), arXiv:1112.0688.
[5] S. Chatrchyan *et al.* (CMS Collaboration), JHEP **1307**, 178 (2013), arXiv:1303.5338.
[6] V. P. Frolov and D. Stojkovic, Phys.Rev.Lett. **89**, 151302

(2002), arXiv:hep-th/0208102; D. Stojkovic, K. Freese, and G. D. Starkman, Phys.Rev. **D72**, 045012 (2005), arXiv:hep-ph/0505026.

[7] A. Flachi and T. Tanaka, Phys. Rev. Lett. **95**, 161302 (2005), arXiv:hep-th/0506145; A. Flachi, O. Pujolas, M. Sasaki, and T. Tanaka, Phys. Rev. **D74**, 045013 (2006), arXiv:hep-th/0604139.

[8] D. Stojkovic, Phys.Rev.Lett. **94**, 011603 (2005), arXiv:hep-ph/0409124.

[9] R. Emparan, A. Fabbri, and N. Kaloper, JHEP **08**, 043 (2002), arXiv:hep-th/0206155.

[10] T. Tanaka, Prog. Theor. Phys. Suppl. **148**, 307 (2003), arXiv:gr-qc/0203082; A. L. Fitzpatrick, L. Randall, and T. Wiseman, JHEP **11**, 033 (2006), arXiv:hep-th/0608208.

[11] T. Tanaka and X. Montes, Nucl. Phys. **B582**, 259 (2000), arXiv:hep-th/0001092.

[12] H. Kudoh, T. Tanaka, and T. Nakamura, Phys. Rev. **D68**, 024035 (2003), arXiv:gr-qc/0301089; H. Kudoh, Prog. Theor. Phys. **110**, 1059 (2004), arXiv:hep-th/0306067.

[13] H. Kudoh, Phys. Rev. **D69**, 104019 (2004), arXiv:hep-th/0401229.

[14] P. Figueras and T. Wiseman, Phys. Rev. Lett. **107**, 081101 (2011), arXiv:1105.2558; S. Abdolrahimi, C. Cattoen, D. N. Page, and S. Yaghoobpour-Tari, Phys. Lett. **B720**, 405 (2013), arXiv:1206.0708.

[15] R. Emparan, G. T. Horowitz, and R. C. Myers, JHEP **0001**, 007 (2000), arXiv:hep-th/9911043.

[16] R. Emparan, G. T. Horowitz, and R. C. Myers, JHEP **0001**, 021 (2000), arXiv:hep-th/9912135.

[17] S. Fraser and D. M. Eardley, (2014), arXiv:1408.4425.

[18] N. Tanahashi and T. Tanaka, Prog. Theor. Phys. **123**, 369 (2010), arXiv:0910.5303.

[19] C. W. Misner, Ann. Phys. **24**, 102 (1963).

[20] R. W. Lindquist, J. Math. Phys. **4**, 938 (1963).

[21] W. Israel, Nuovo Cim. **B44S10**, 1 (1966).

[22] S. Fraser and D. M. Eardley, (2014), arXiv:1408.6586.

[23] N. T. Bishop, Gen. Rel. Grav. **14**, 717 (1982).

[24] A. Chamblin, S. Hawking, and H. Reall, Phys. Rev. **D61**, 065007 (2000), arXiv:hep-th/9909205.

[25] E. G. Adelberger, B. R. Heckel, S. A. Hoedl, C. Hoyle, D. Kapner, *et al.*, Phys. Rev. Lett. **98**, 131104 (2007), arXiv:hep-ph/0611223.

[26] R. Emparan, Phys. Rev. **D64**, 024025 (2001), arXiv:hep-th/0104009.

[27] L. A. Anchordoqui, H. Goldberg, and A. D. Shapere, Phys. Rev. **D66**, 024033 (2002), arXiv:hep-ph/0204228.